



Medical Image Reconstruction Term II – 2012

Topic 3: Image Reconstruction in the Fourier Domain

Professor Yasser Mostafa Kadah

Topics Today

- ▶ Reconstruction from Uniformly Sampled k-Space
- ▶ Projection-slice theorem
- ▶ Interlaced Fourier transform
- ▶ Partial Fourier Methods
- ▶ Reconstruction from Nonuniformly Sampled k-Space



Reconstruction from k-Space Samples

- ▶ Several imaging modalities produce data in k-space
 - ▶ Computed Tomography (CT): radial sampling
 - ▶ Magnetic Resonance Imaging (MRI): several sampling strategies are used such as radial, spiral, and random sampling
- ▶ Main Reconstruction Method: Compute Inverse 2D DFT to compute the image!

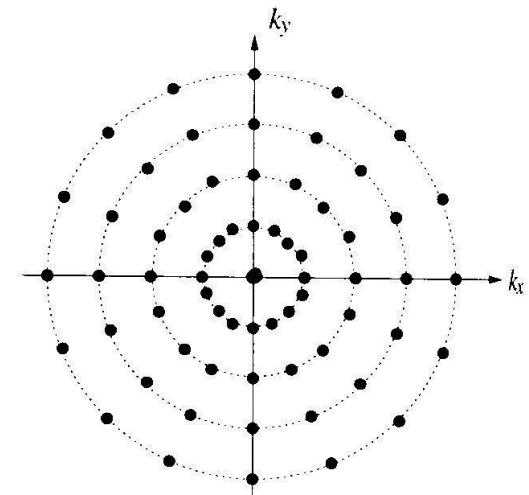
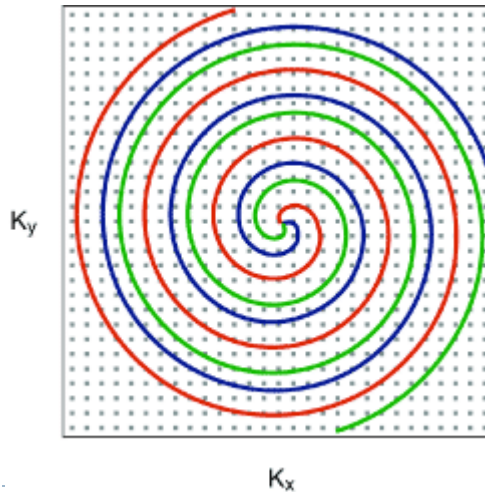
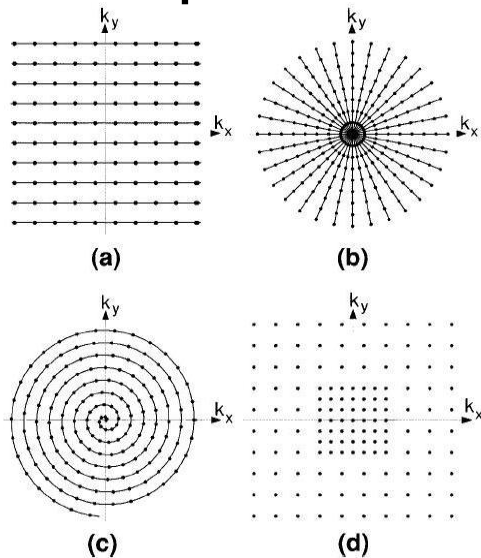
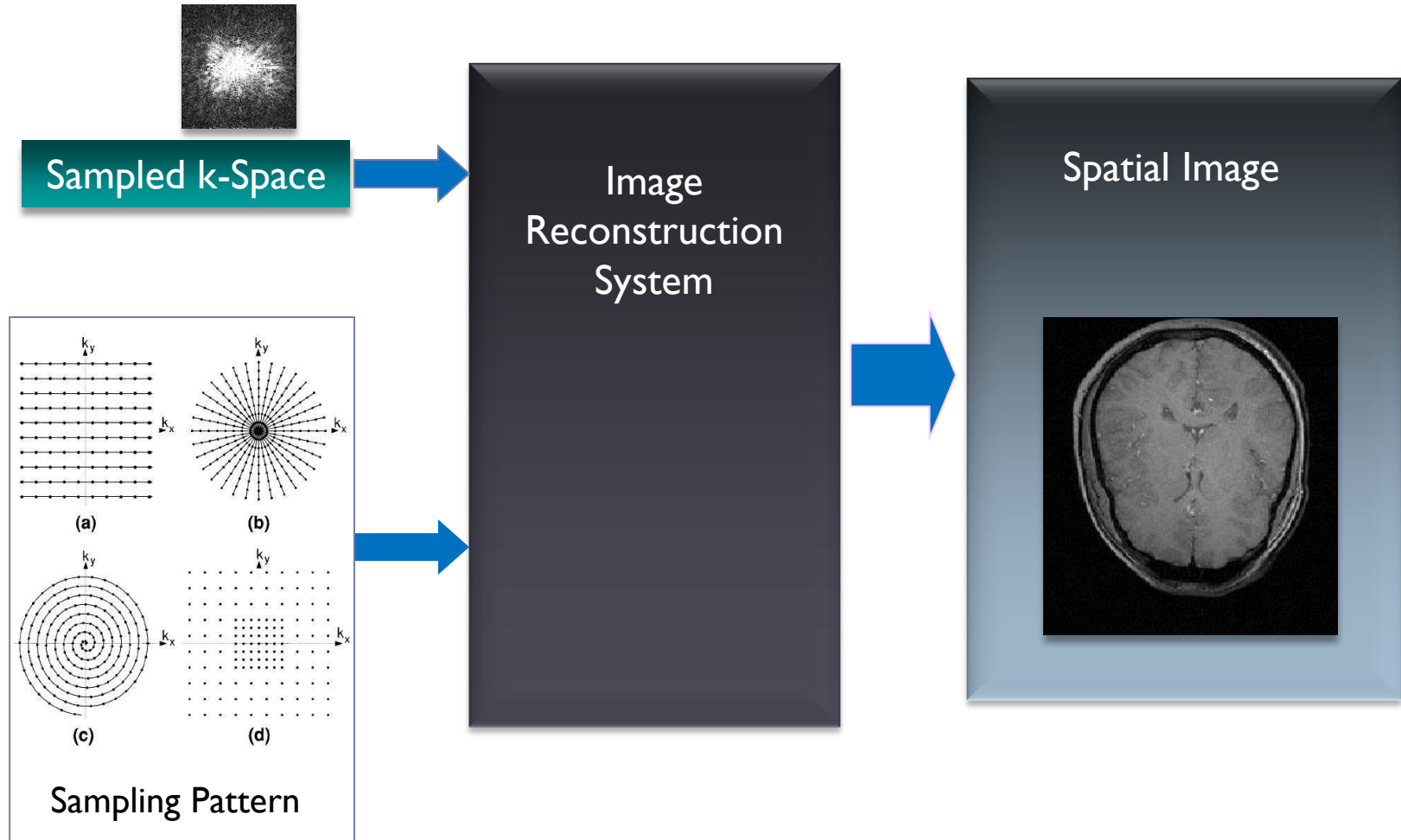
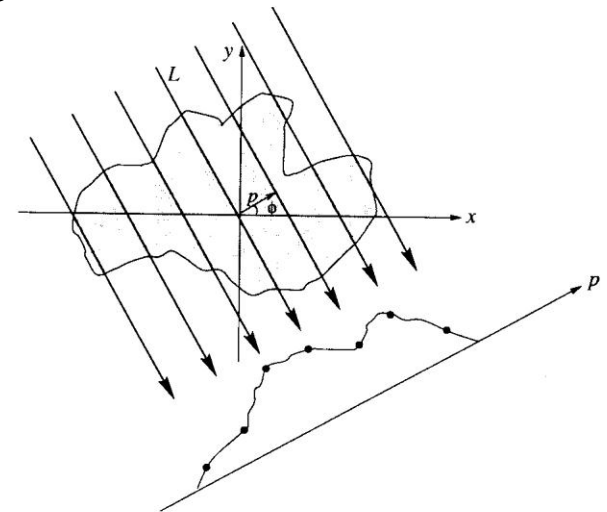


Image Reconstruction Problem

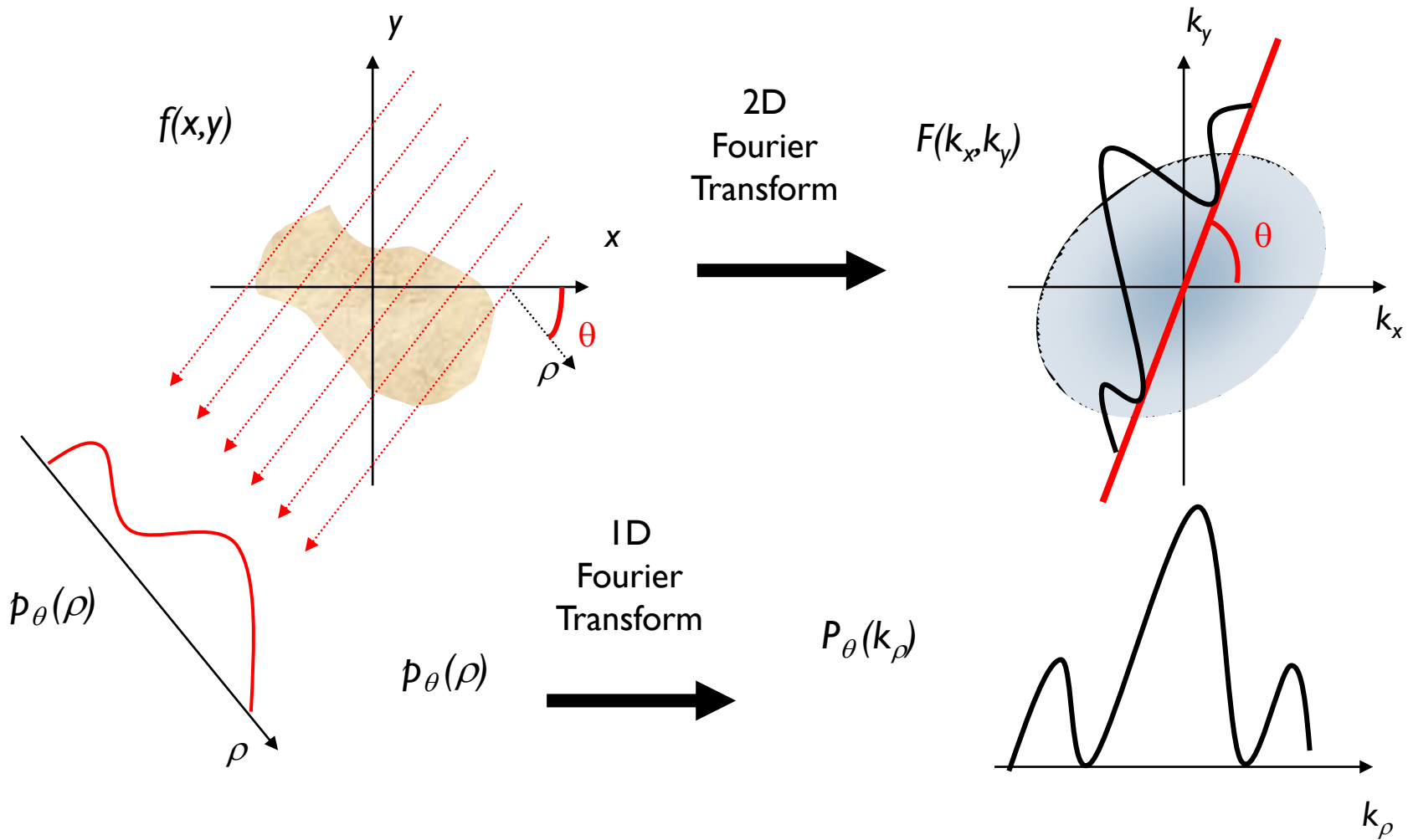


Projection-Slice Theorem

- ▶ Also known as Central-Slice Theorem
- ▶ A property of the Fourier transform
- ▶ Relates the projection data in the spatial domain to the frequency domain
- ▶ States that the 1D Fourier transform of the projection of an image at an angle θ is equal to the slice of the 2D Fourier transform at the same angle



Projection-Slice Theorem



Projection-Slice Theorem

- ▶ 2D Fourier transformation:

$$F(k_x, k_y) = \iint f(x, y) \cdot e^{-j2\pi(k_x \cdot x + k_y \cdot y)} dx dy$$

- ▶ The slice of the 2D Fourier transform at $k_x=0$ is given by:

$$F(0, k_y) = \int \left(\int f(x, y) dx \right) \cdot e^{-j2\pi k_y \cdot y} dy$$

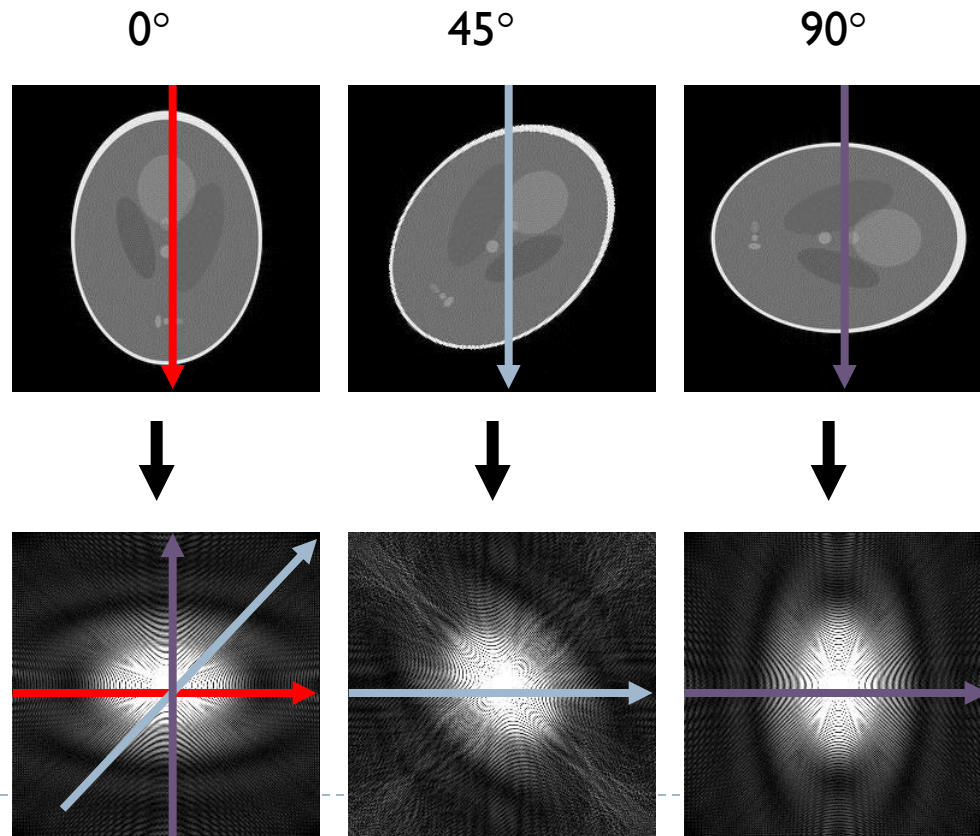
and at $k_y=0$ is given by

$$F(k_x, 0) = \int \left(\int f(x, y) dy \right) \cdot e^{-j2\pi k_x \cdot x} dx$$



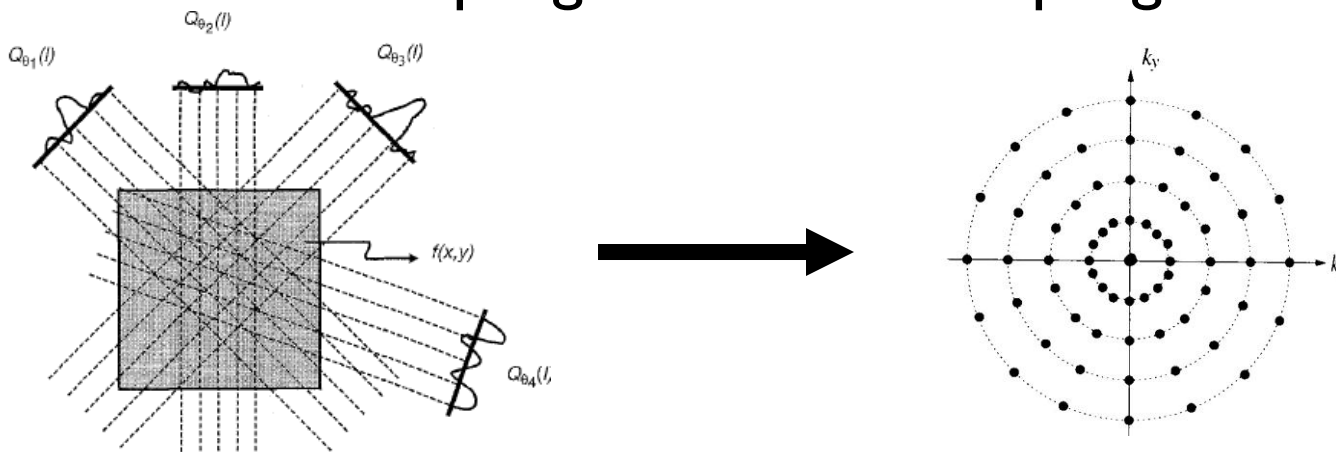
Projection-Slice Theorem

- ▶ For a general angle, the rotation property of the Fourier transformation can be used to generalize the mathematical result for a vertical projection to any angle



Projection-Slice Theorem: Application to CT

- ▶ The projection data can be shown to correspond to radial sampling of the frequency domain
- ▶ It is not straightforward to numerically compute the image from this frequency domain representation
 - ▶ Limitation of the DFT to uniform sampled data
- ▶ Interpolation can be used in the frequency domain to re-grid the radial sampling to uniform sampling



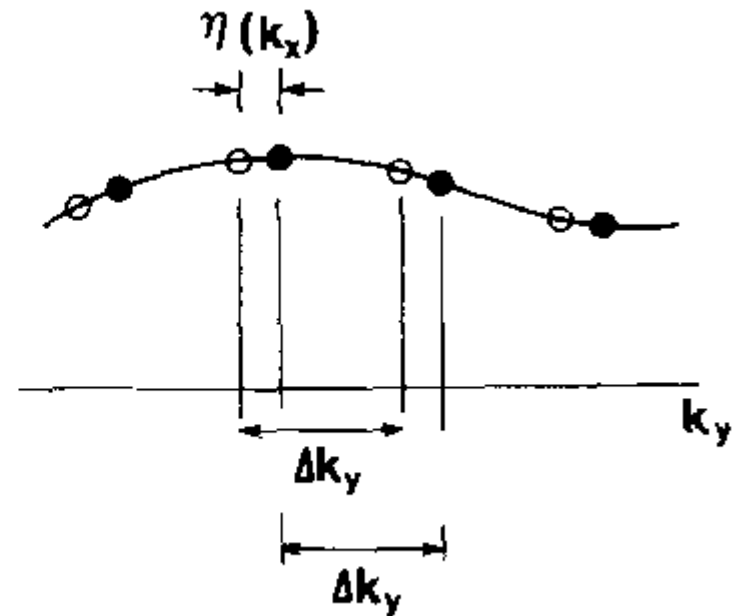
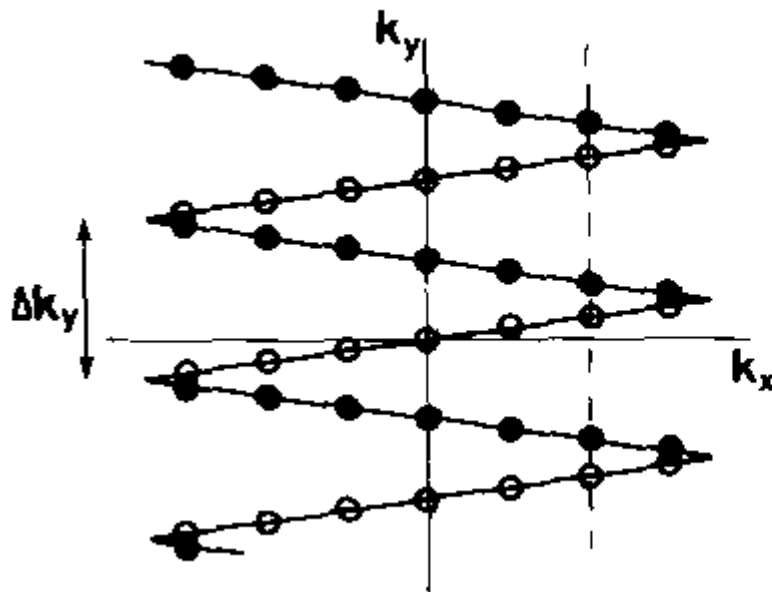
Projection-Slice Theorem: Application to MRI

- ▶ Navigator echo motion estimation
 - ▶ Acquire a single k-space line in the middle to estimation linear translation in this direction
- ▶ Early MRI reconstruction based on backprojection algorithms



Interlaced Fourier Transform

- ▶ A special case of nonuniform Fourier transform



Interlaced Fourier Transform

► Mathematical formulation

$$g(k_x, y) = \frac{-e^{\kappa 2\pi i \xi(k_x)}}{1 - e^{\kappa 2\pi i \xi(k_x)}} g_P(k_x, y) + \frac{e^{iy\eta(k_x)}}{1 - e^{\kappa 2\pi i \xi(k_x)}} g_N(k_x, y),$$

$$h(k_x, y) = \frac{1}{1 - e^{\kappa 2\pi i \xi(k_x)}} g_P(k_x, y) - \frac{e^{iy\eta(k_x)}}{1 - e^{\kappa 2\pi i \xi(k_x)}} g_N(k_x, y),$$

$$G(k_x, y) = h\left(k_x, y + \frac{L_y}{2}\right) \quad -\frac{L_y}{2} \leq y < -\frac{L_y}{4}$$

$$G(k_x, y) = g(k_x, y) \quad -\frac{L_y}{4} \leq y \leq \frac{L_y}{4}$$

$$G(k_x, y) = h\left(k_x, y - \frac{L_y}{2}\right) \quad \frac{L_y}{4} < y \leq \frac{L_y}{2}$$

Interlaced Fourier Transform

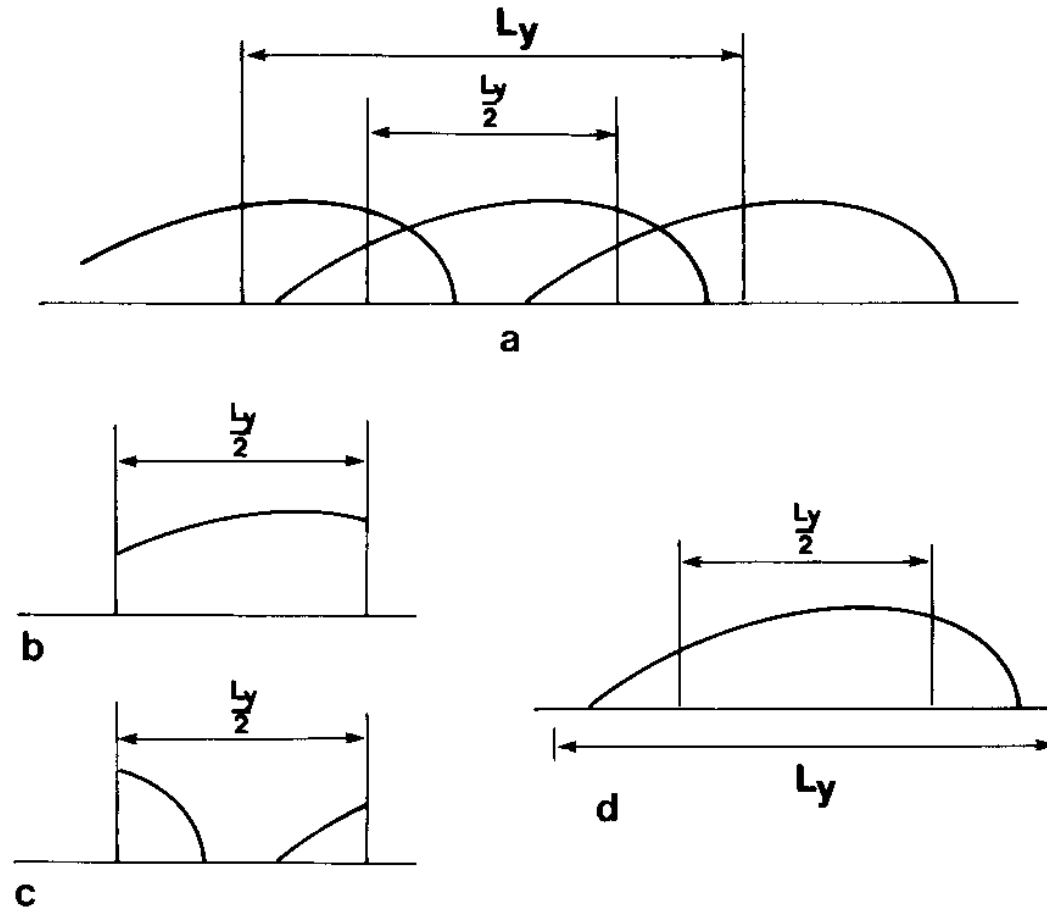


FIG. 2. (a) $g_p(k_x, y)$ at a specific k_x . (b) $g(k_x, y)$ at same k_x as in (a). (c) $h(k_x, y)$ at same k_x as in (a). (d) $G(k_x, y)$ at same k_x as in (a), (b), and (c).

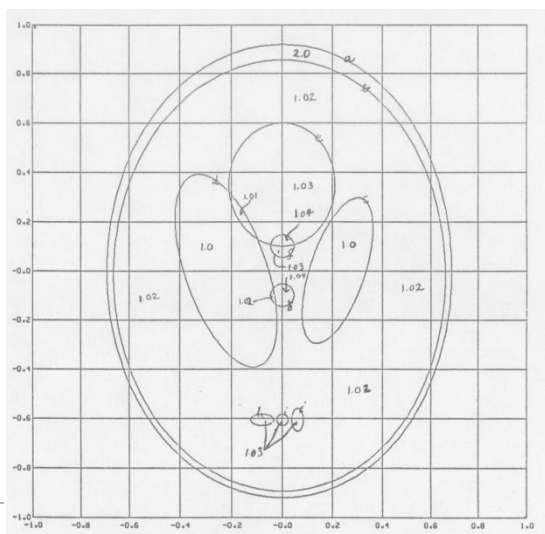


Shepp-Logan Phantom

- ▶ Numerical phantom used to simulate the human head to evaluate reconstruction algorithms in computed tomography

RECONSTRUCTING INTERIOR HEAD TISSUE
FROM X-RAY TRANSMISSIONS

L. A. Shepp and B. F. Logan
Bell Laboratories
Murray Hill, New Jersey 07974



Shepp-Logan Phantom

TABLE 1

<u>Ellipses</u>	<u>Center</u>	<u>Major Axis</u>	<u>Minor Axis</u>	<u>Theta</u>	<u>Gray level</u>
a	(0,0)	.69	.92	0	2
b	(0,-.0184)	.6624	.874	0	-.98
c	(.22,0)	.11	.31	-18°	-.02
d	(-.22,0)	.16	.41	18°	-.02
e	(0,.35)	.21	.25	0	.01
f	(0,.1)	.046	.046	0	.01
g	(0,-.1)	.046	.046	0	.02
h	(-.08,-.605)	.046	.023	0	.01
i	(0,-.605)	.023	.023	0	.01
j	(.06,-.605)	.023	.046	0	.01

Shepp-Logan Phantom: 3D

Table 1: 3D Shepp-Logan Phantom Specification for MRI

Ellipsoid (i)	Center (r_0)			Half-Axis			Angle	Spin Density	Portion Subtracted	Tissue Type
	x	y	z	a	b	c	\square			
1*	0	0	0	0.72	0.95	0.93	0	0.8	None	Scalp
2	0	0	0	0.69	0.92	0.9	0	0.12 [13]	2[Prop[1]]	Bone & Marrow
3*	0	-0.0184	0	0.6624	0.874	0.88	0	0.98 [13]	3[Prop[2]]	CSF
4**	0	-0.0184	0	0.6524	0.864	0.87	0	0.745 [14]	4[Prop[3]]	Gray Matter
5	-0.22	0	-0.25	0.41	0.16	0.21	-72°	0.98	5[Prop[4]]	CSF
6	0.22	0	-0.25	0.31	0.11	0.22	72°	0.98	6[Prop[4]]	CSF
7	0	0.35	-0.25	0.21	0.25	0.35	0	0.617 [14]	7[Prop[4]]	White Matter
8	0	0.1	-0.25	0.046	0.046	0.046	0	0.95 [6]	8[Prop[4]]	Tumor
9	-0.08	-0.605	-0.25	0.046	0.023	0.02	0	0.95	9[Prop[4]]	Tumor
10	0.06	-0.605	-0.25	0.046	0.023	0.02	-90°	0.95	10[Prop[4]]	Tumor
11	0	-0.1	-0.25	0.046	0.046	0.046	0	0.95	11[Prop[4]]	Tumor
12	0	-0.605	-0.25	0.023	0.023	0.023	0	0.95	12[Prop[4]]	Tumor
13†*	0.06	-0.105	0.0625	0.056	0.04	0.1	-90°	0.93 [6]	13[Prop[4]]	Tumor
14†*	0	0.1	0.625	0.056	0.056	0.1	0	0.98	14[Prop[4]]	CSF
15††	0.56	-0.4	-0.25	0.2	0.03	0.1	70°	0.85 [15]	Not Used	Blood Clot

* Regions that were not in original Shepp-Logan (S-L) phantom, ** Slightly modified from original S-L phantom, †3D phantom only, †† Optional region for original S-L phantom, not used herein. Portion subtracted: e.g., 2[Prop[1]] means we subtract an ellipsoid with Ellipsoid 2's geometry (center and dimensions) but Ellipsoid 1's MR properties (relaxation and spin density). Scalp spin density is based on muscle/fat water content since skin water content is highly variable. Tumor spin density is based on its x-ray attenuation coefficient [6].

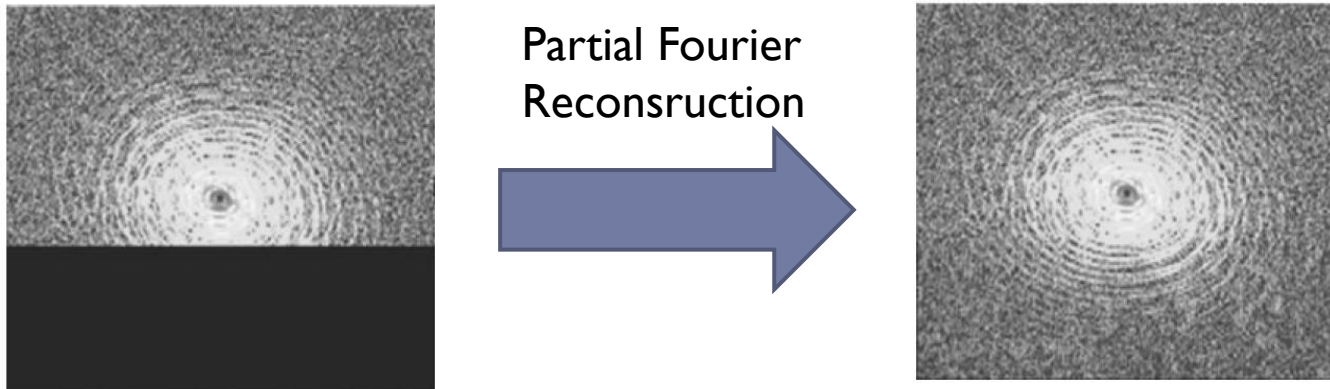
Shepp-Logan Phantom: k-Space

- ▶ Using the known Fourier transformation of the Shepp-Logan phantom components (circles and ellipses), one can generate the analytical form of its Fourier transformation
 - ▶ Can be sampled arbitrarily to generate uniformly or nonuniformly sampled data for close to real data generation
 - ▶ Applications include radial sampling (e.g., CT and MRI), spiral and random sampling (MRI).
- ▶ This will be the standard for all evaluation procedures of image reconstruction methods.



Partial Fourier Reconstruction

- ▶ PF reconstruction is based on the fact that if the object is real in image space, its Fourier transform is Hermitian.
 - ▶ *One-half of the k -space is needed to reconstruct a real image*
- ▶ In reality, however, the reconstructed images are complex.



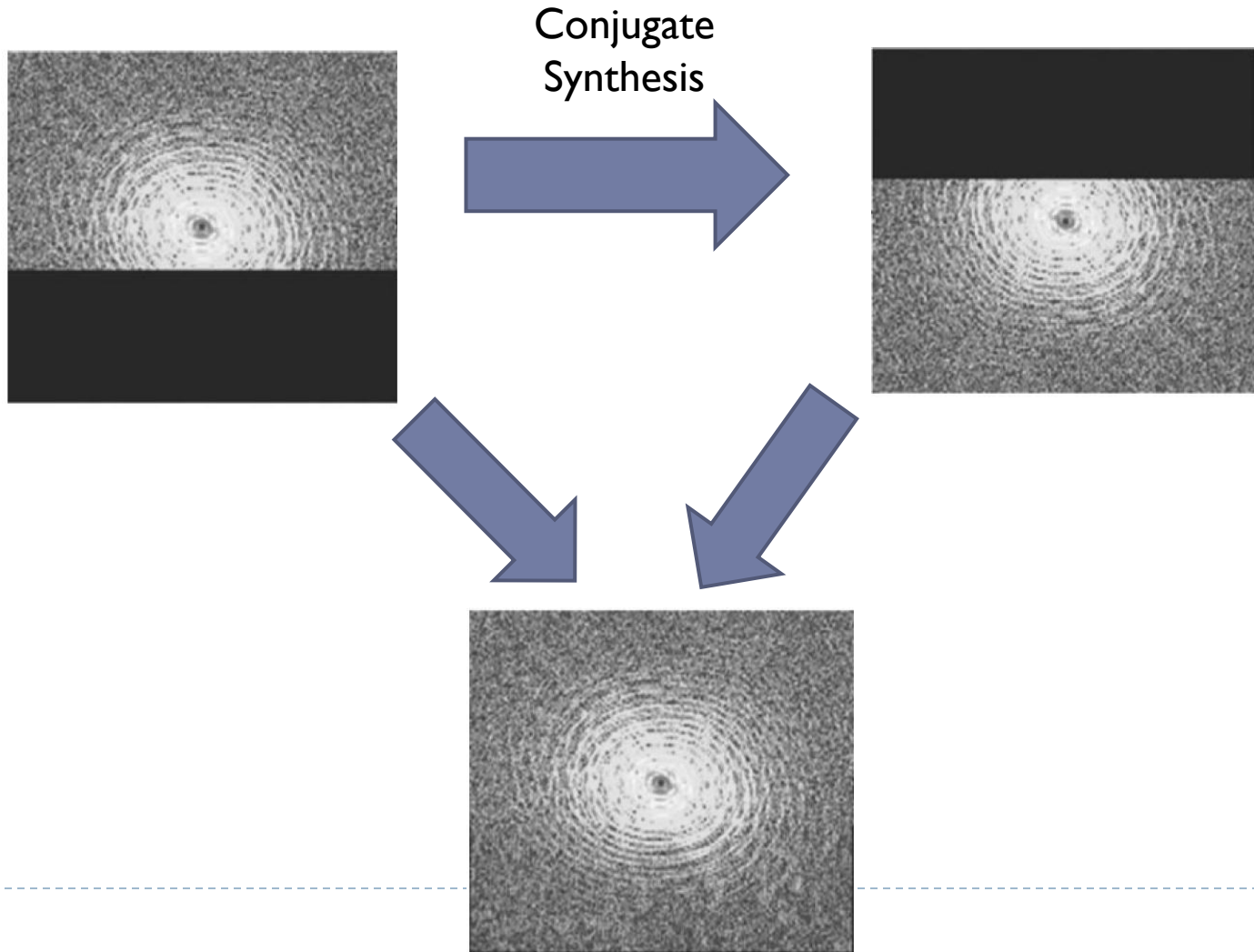
Quantitative Evaluation of Several Partial Fourier Reconstruction Algorithms Used in MRI

G. McGibney, M. R. Smith, S. T. Nichols, A. Crawley

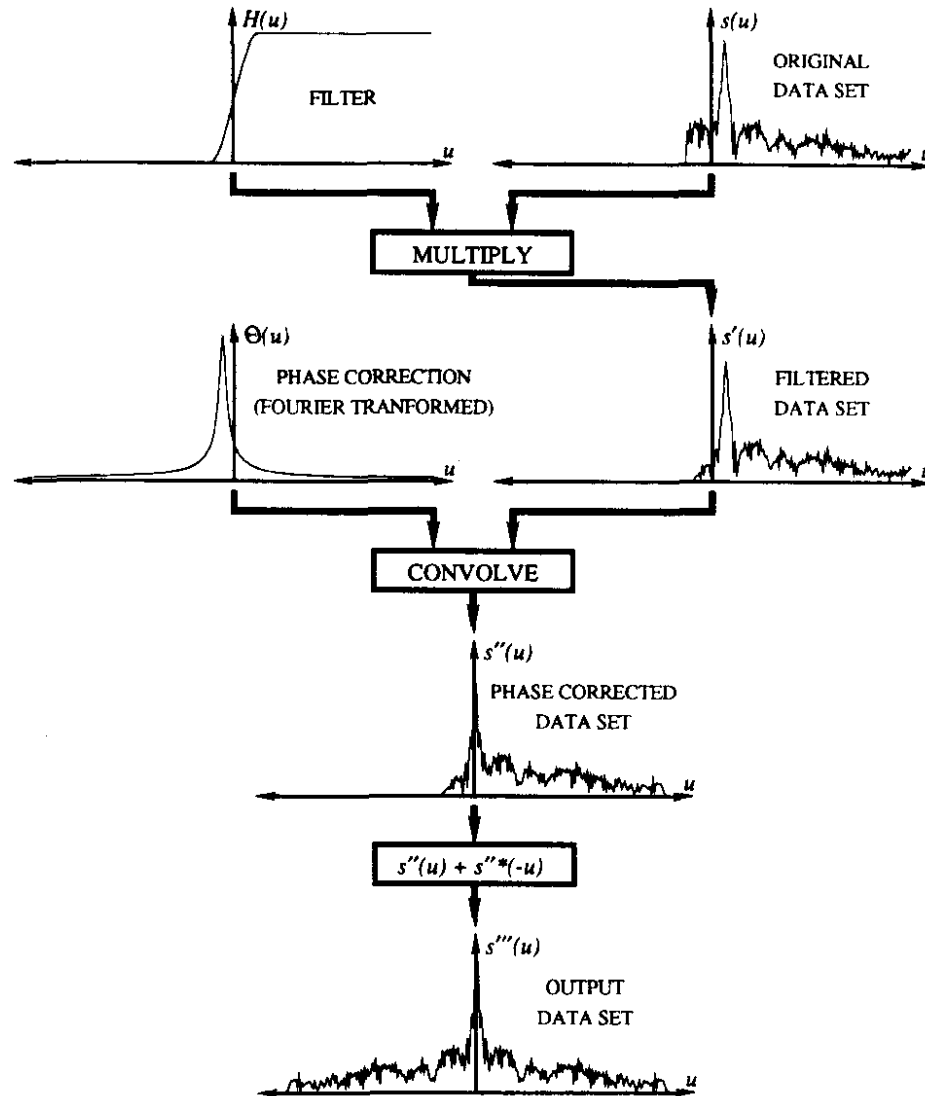
MRM 30:51–59 (1993)

Conjugate Synthesis

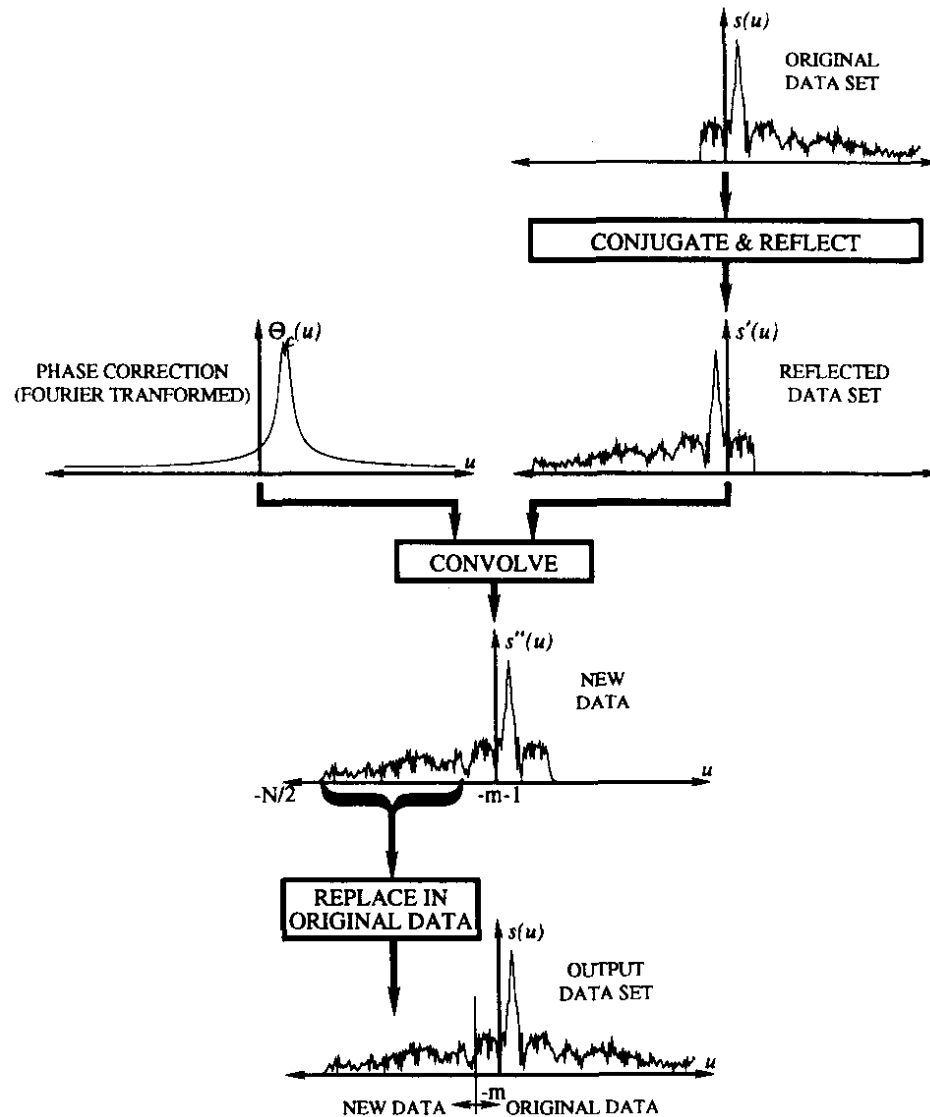
- ▶ Assume image is purely real



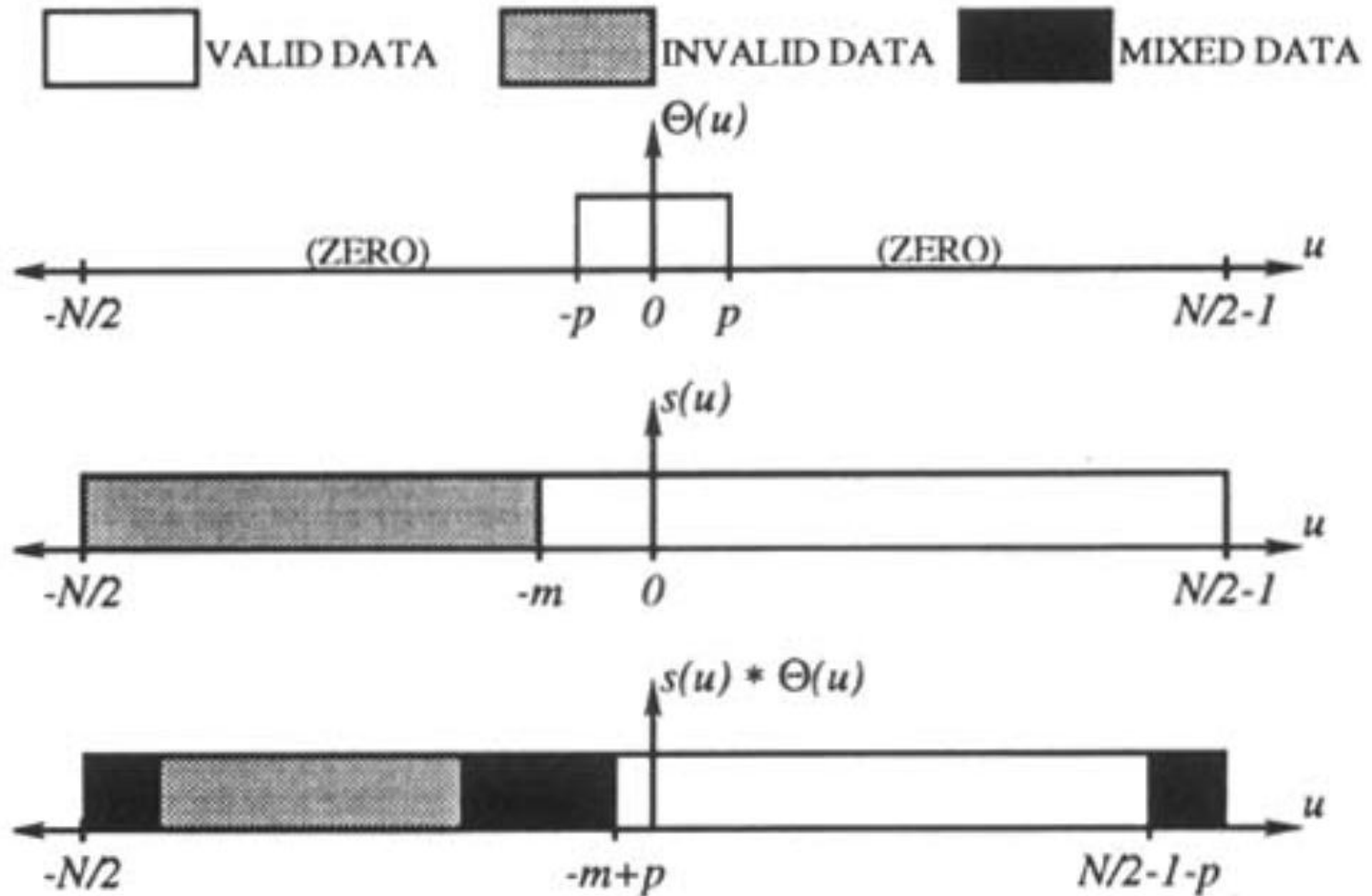
Margosian Method



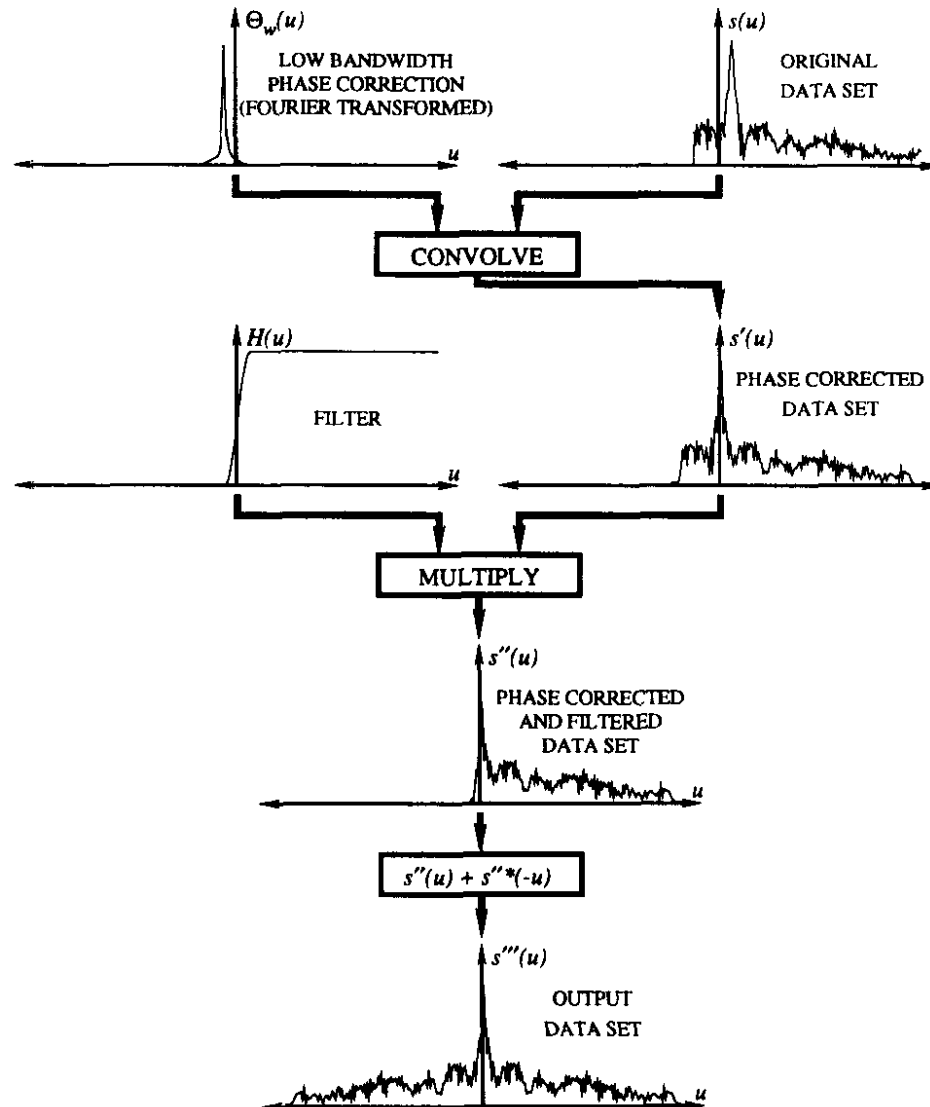
Cuppen/POCS Method



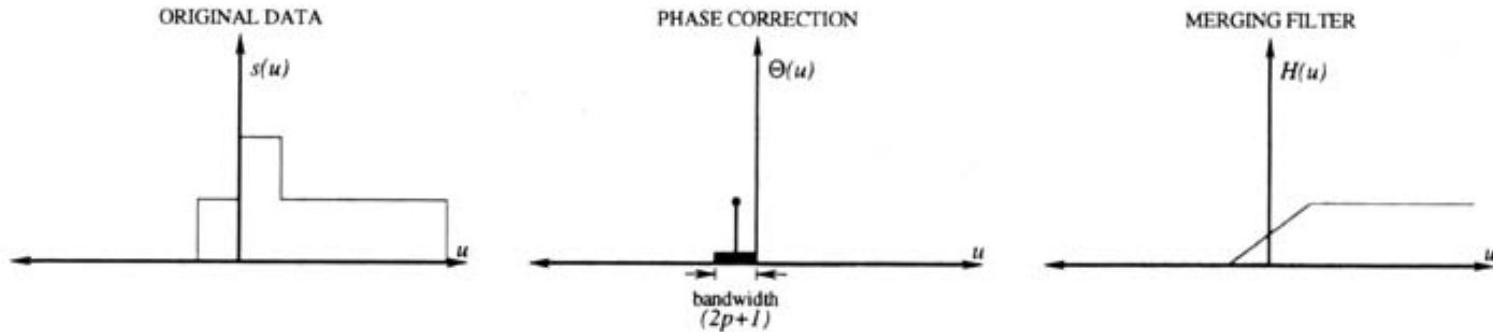
Phase Correction Effects



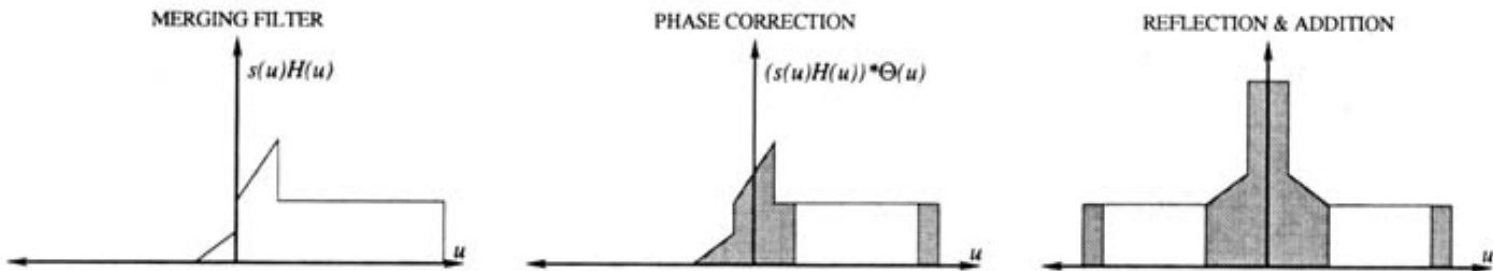
FIR and MoFIR Methods



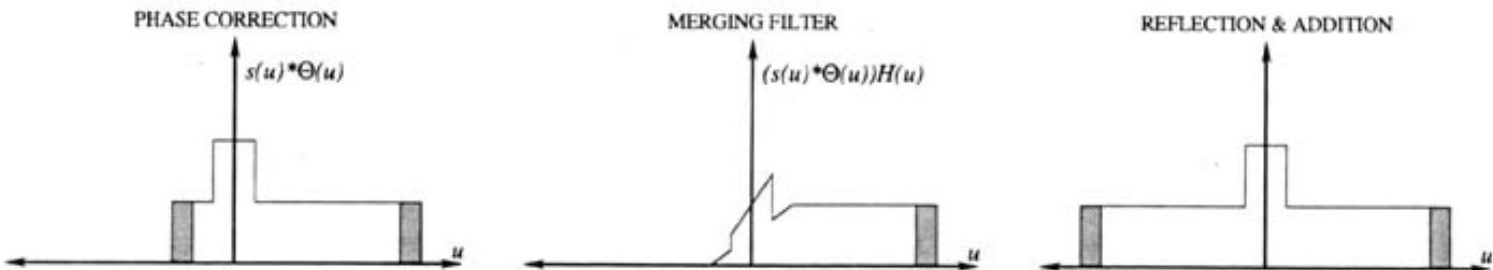
Comparison of Distortions in Margosian and MoFIR Methods



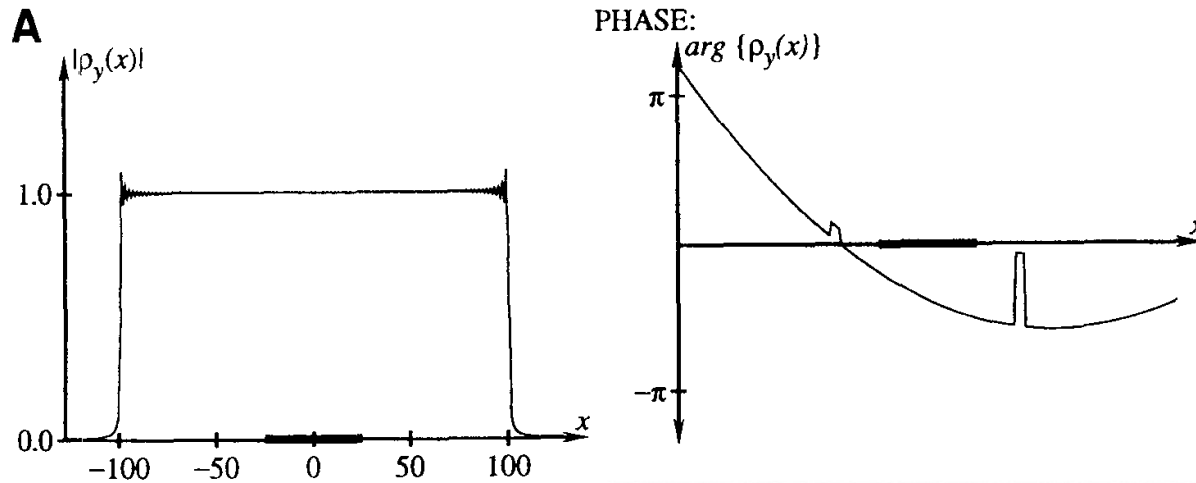
MARGOSIAN RECONSTRUCTION



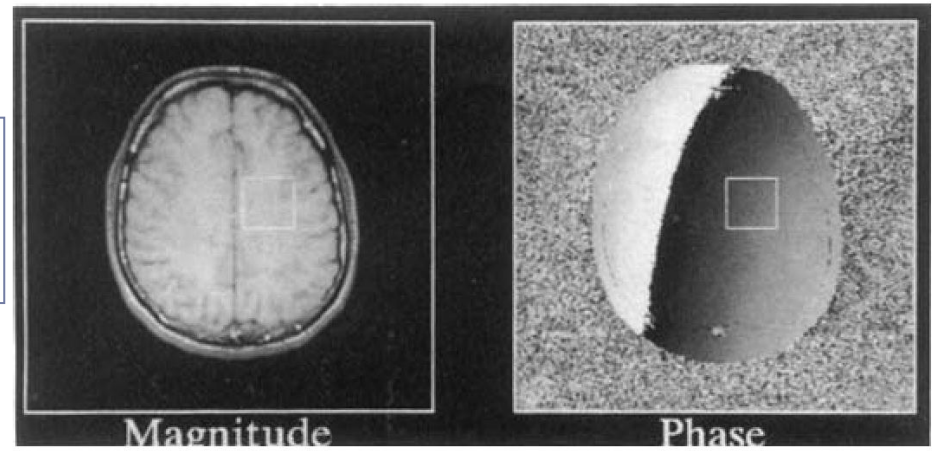
MoFIR RECONSTRUCTION



Experimental Verification: Simulated Box and Real Data

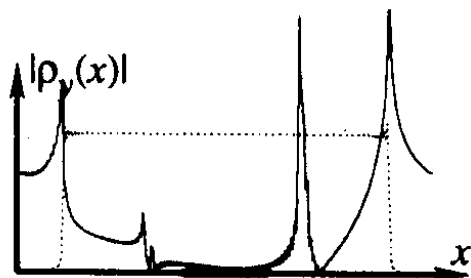


$$\text{error} = \frac{\sum_{(x,y) \in R} (|\rho_{\text{partial}}| - |\rho_{\text{full}}|)^2}{\sum_{(x,y) \in R} (|\rho_{\text{full}}|)^2} \cdot 100\%$$



Results

CONJUGATE SYNTHESIS



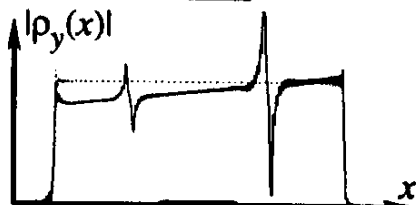
GE=89.3% LE=92.7%

EXACT ESTIMATE

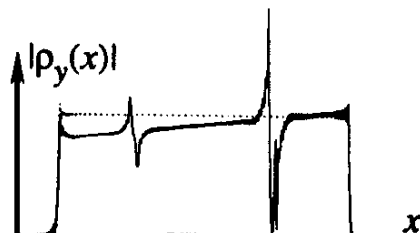
GE = GLOBAL ERROR
LE = LOCAL ERROR

INCORRECT ESTIMATE

MARGOSIAN

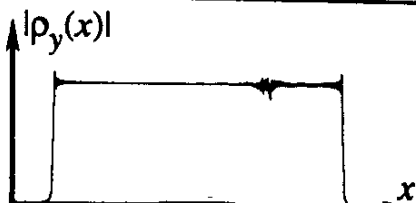


GE=2.79% LE=0.640%

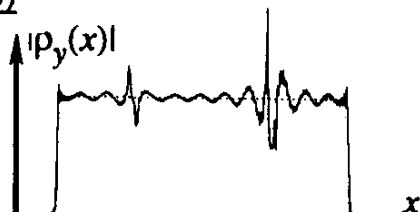


GE=3.48% LE=0.650%

CUPPEN (4 ITERATIONS)

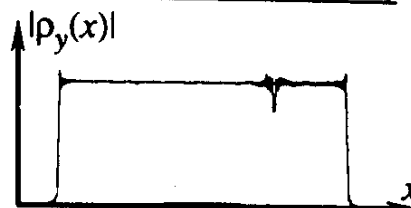


GE=.026% LE=0.001%

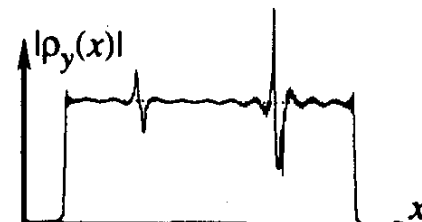


GE=0.986% LE=0.067%

POCS (4 ITERATIONS)

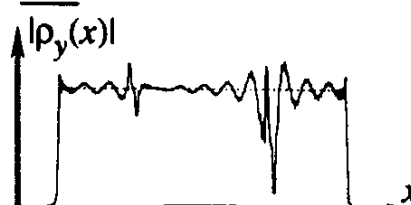


GE=0.072% LE=0.001%

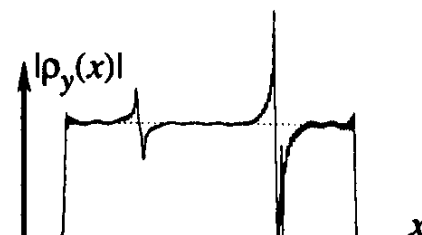


GE=1.148% LE=0.019%

FIR



GE=1.767% LE=0.097%

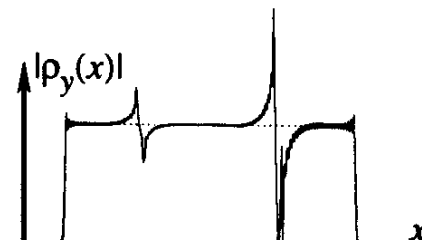


GE=2.722% LE=0.004%

MoFIR

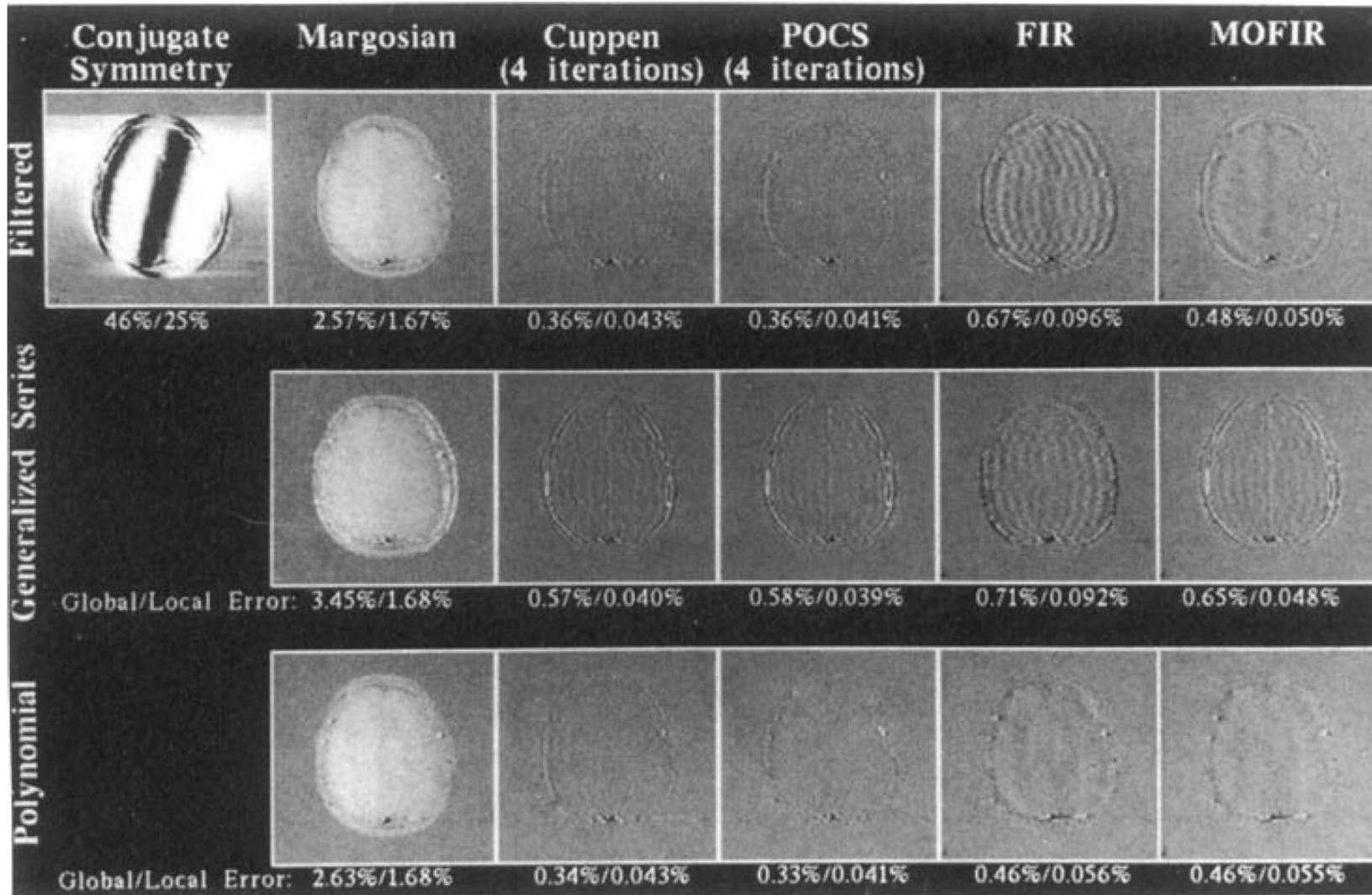


GE=0.437% LE=0.001%



GE=2.734% LE=0.003%

Results



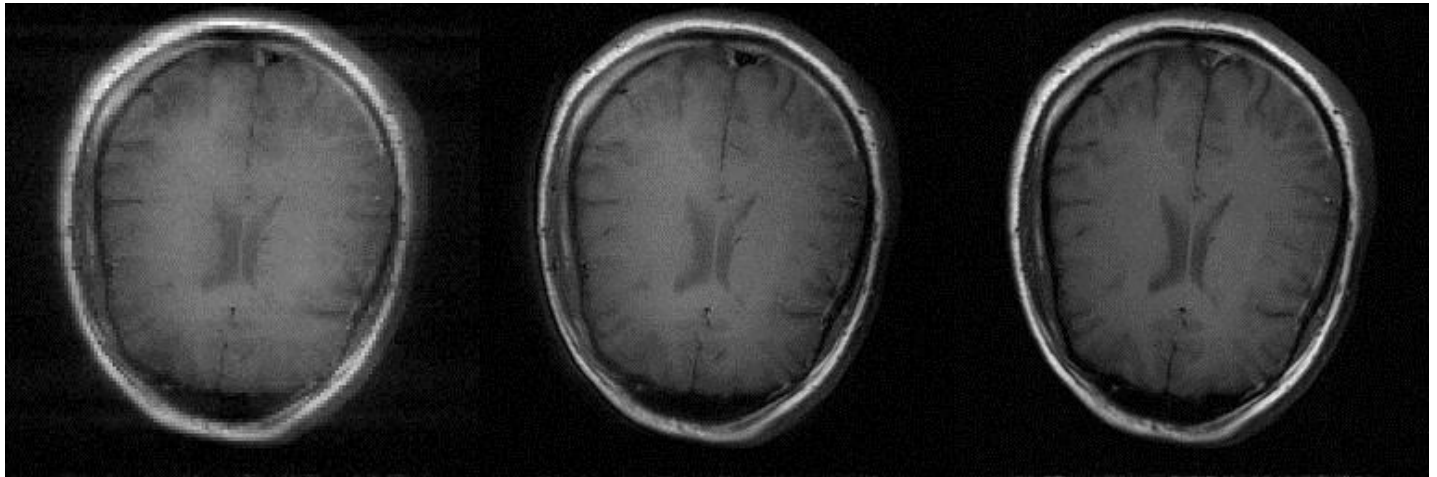
Results

Comparison of the Times of the Partial Fourier Reconstruction Algorithms Both Individually and in Conjunction with the Phase Estimation Algorithms

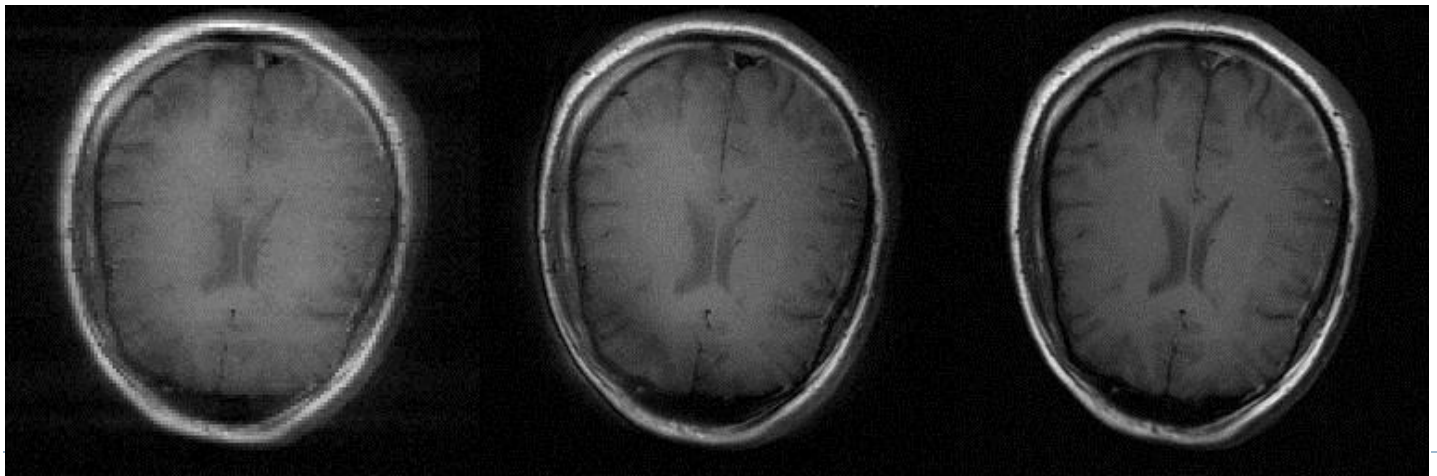
	Partial Fourier only (s)	Partial Fourier plus filtered estimate (s)	Partial Fourier plus generalized series estimate (s)	Partial Fourier plus polynomial estimate (s)
Conjugate-symmetry	2.4	7.1	464	7.1
Margosian-homodyne	2.9	7.6	464	7.6
Cuppen (4 iterations)	12.5	17.2	474	17.2
POCS (4 iterations)	14.6	19.3	476	19.3
<i>FIR</i> (direct)	9.6	14.3	471	14.3
<i>FIR</i> (circular)	5.3	10.0	467	10.0
<i>MoFIR</i> (circular)	5.3	10.0	467	10.0

Results

- ▶ 256x256 image, 16 Lines

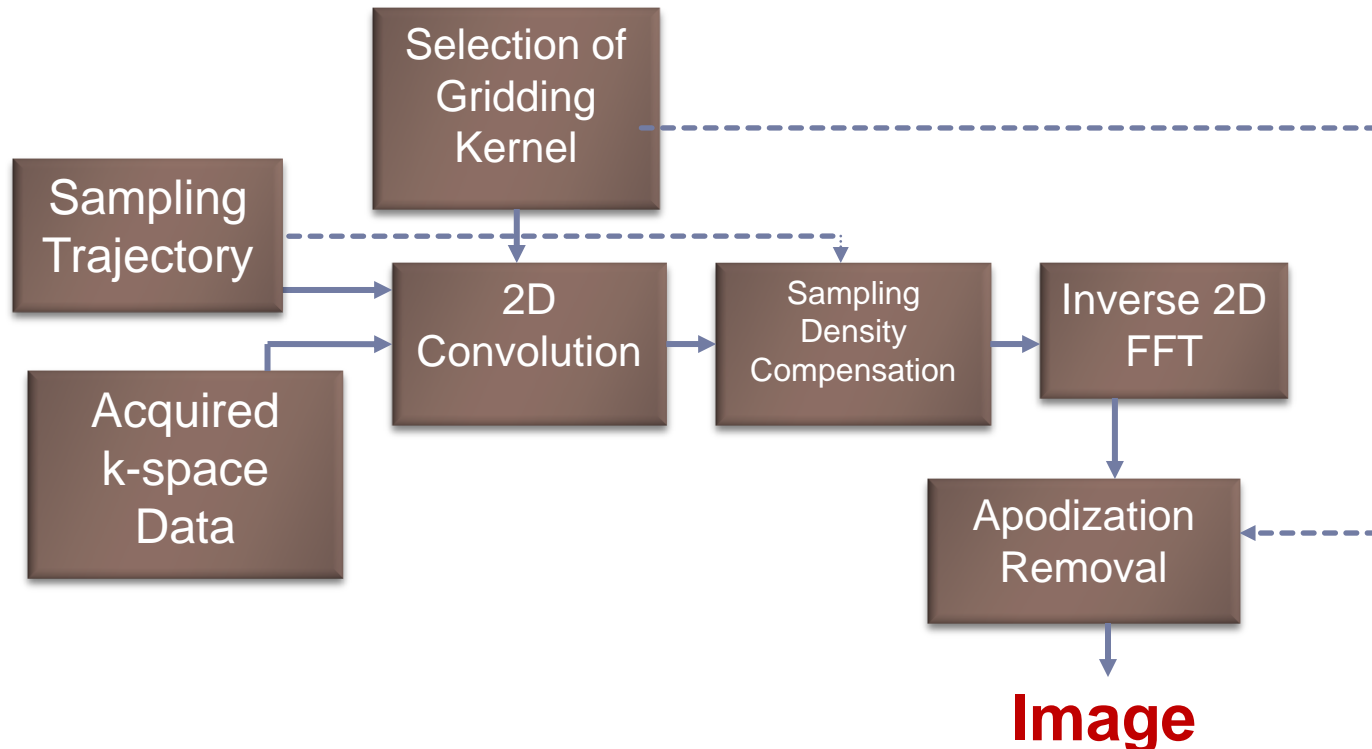


- ▶ 8 Lines



Reconstruction from Nonuniformly Sampled k-space: Conventional Gridding

- ▶ Conventional gridding through convolution with interpolation kernel (O'Sullivan, 1985; Jackson et al., 1991; Meyer et al., 1992)



Meyer Gridding Algorithm

Fast Spiral Coronary Artery Imaging

CRAIG H. MEYER,* BOB S. HU,† DWIGHT G. NISHIMURA,
AND ALBERT MACOVSKI‡

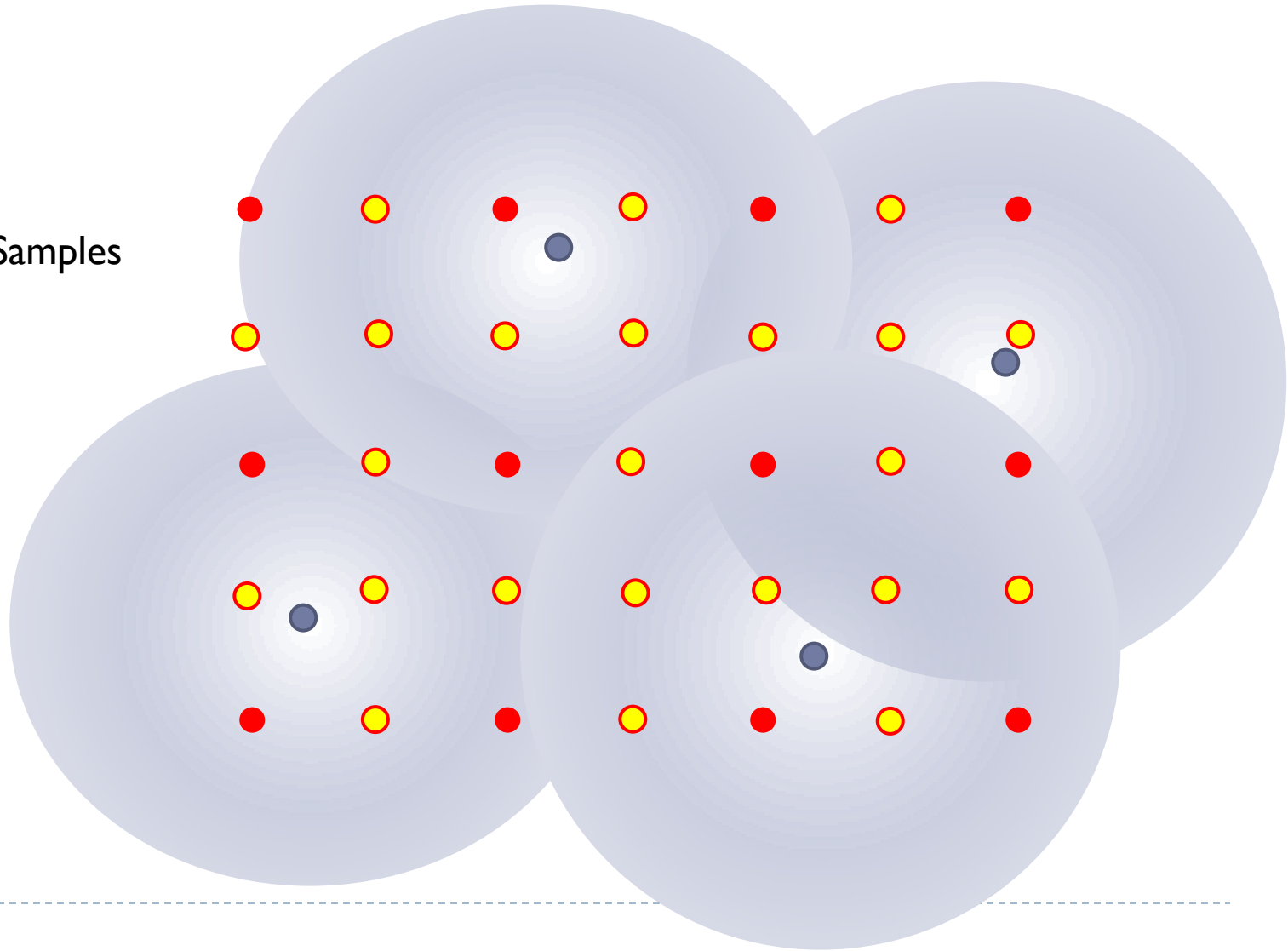
4. Convolve the data into the 2D array. This is done by multiplying each density-compensated data point by a Kaiser–Bessel window a few grid points in width, evaluating the result at each grid point within the window, and adding the result into the array. An auxiliary array is used to keep track of the amount of energy put into each grid point, which is the product of the density-compensation factor and the Kaiser–Bessel function evaluation.
 5. Normalize the energy in each grid point by dividing by the auxiliary array. If the density compensation of step 3 is done properly, this step results in only a minor correction.
 6. Perform a complex 2D FFT.
 7. Divide by the transform of the Kaiser–Bessel window to remove the apodization resulting from the convolution of step 4.
 8. Take the magnitude of the result.
-
- 

Meyer Gridding Algorithm

● Nonuniform Samples

● 1x Grid

● 2x Grid



Jackson Gridding Window Selection

Selection of a Convolution Function for Fourier Inversion Using Gridding

John I. Jackson, Craig H. Meyer, Dwight G. Nishimura, *Member, IEEE*, and Albert Macovski, *Fellow, IEEE*

TABLE I
THE PARAMETER VALUES FOR EACH FUNCTION TYPE THAT PROVIDE THE
LEAST RELATIVE ALIASED ENERGY WHEN GRIDDING ONTO A REGULAR GRID

Window Width	Two-Term cos α	Three-Term cos		Gaussian σ	Kaiser-Bessel β
		α	β		
1.5	0.7600	0.8701	0.2311	0.4241	1.9980
2.0	0.7146	0.8099	0.3108	0.4927	2.3934
2.5	0.6185	0.6932	0.4176	0.4839	3.3800
3.0	0.5534	0.5995	0.4675	0.5063	4.2054
3.5	0.5185	0.5383	0.4831	0.5516	4.9107
4.0		0.4998	0.4891	0.5695	5.7567
4.5		0.4653	0.4972	0.5682	6.6291
5.0		0.4463	0.4985	0.5974	7.4302

Jackson's Gridding Window Selection

TABLE II
THE PARAMETER VALUES FOR EACH FUNCTION TYPE THAT PROVIDE THE
LEAST RELATIVE ALIASED ENERGY WHEN GRIDDING ONTO A $2 \times$
SUBSAMPLED GRID

Window Width	Two-Term cos α	Three-Term cos		Gaussian σ	Kaiser-Bessel β
		α	β		
1.5	0.5273	0.4715	0.4917	0.2120	6.6875
2.0	0.5125	0.4149	0.4990	0.2432	9.1375
2.5	0.5076	0.4011	0.4996	0.2691	11.5250
3.0	0.5068	0.3954	0.4997	0.2920	13.9086
3.5	0.5051	0.3897	0.4999	0.3145	16.2734
4.0		0.3850	0.5000	0.3363	18.5547
4.5		0.3833	0.5000	0.3557	
5.0		0.3823	0.5000	0.3737	

Disadvantages of Gridding Methods

- ▶ Reconstructed images do not represent optimality in any sense
- ▶ Variation of performance with form of k-space trajectory
- ▶ Lack of explicit methodology to trade-off accuracy and speed of reconstruction
- ▶ Not possible to progressively improve the accuracy of reconstruction



Kadah's Method

Progressive Magnetic Resonance Image Reconstruction Based on Iterative Solution of a Sparse Linear System

Yasser M. Kadah,^{1,2} Ahmed S. Fahmy,^{2,3} Refaat E. Gabr,^{2,3} Keith Heberlein,¹ and Xiaoping P. Hu¹

- ▶ Algebraic Solution
- ▶ Iterative reconstruction method that provides an optimal solution in the least-squares sense
- ▶ Based on a practical imaging model
- ▶ Progressive reconstruction capability
- ▶ Simple mechanism to control trade-off between accuracy and speed



Theory

- ▶ Assume a piecewise constant spatial domain representing display using pixels
 - ▶ Image composed of pixel each of uniform intensity
 - ▶ Image can be represented by a sum of 2D RECT functions
- ▶ Assume spatial domain to be compact
 - ▶ Field of view is always finite in length
- ▶ The image can be expressed in terms of gate functions as,

$$f(x, y) = \sum_{n=0}^{N-1} \sum_{m=0}^{M-1} \alpha_{n,m} \cdot \Pi(x - x_n, y - y_m)$$



Theory

- ▶ Applying **continuous Fourier transform**,

$$F(k_x, k_y) = \int_{-\infty}^{\infty} \int_{-\infty}^{\infty} \sum_{n=0}^{N-1} \sum_{m=0}^{M-1} \alpha_{n,m} \cdot \Pi(x - x_n, y - y_m) \cdot e^{-j2\pi(k_x x + k_y y)} dx dy,$$

- ▶ Hence,

$$F(k_x, k_y) = \text{Sinc}(w_x k_x) \cdot \text{Sinc}(w_y k_y) \sum_{n=0}^{N-1} \sum_{m=0}^{M-1} \alpha_{n,m} \cdot e^{-j2\pi(k_x x_n + k_y y_m)}.$$

- ▶ This can be expressed in the form of a linear system as

$$\mathbf{b} = \mathbf{A}\mathbf{v}$$

- ▶ A matrix is $\sim N^2 \times N^2$ and complex-valued
-



Theory

- ▶ Observation: A matrix is $\sim N^2 \times N^2$ and complex-valued
 - ▶ Solve a $|6384 \times 6384$ linear system to get a $|28 \times 28$ image
 - ▶ Very difficult to solve in practice because of size

$$\begin{aligned}
 & \begin{bmatrix} \frac{F(k_x^0, k_y^0)}{\text{Sinc}(w_x k_x^0) \cdot \text{Sinc}(w_y k_y^0)} \\ \frac{F(k_x^1, k_y^1)}{\text{Sinc}(w_x k_x^1) \cdot \text{Sinc}(w_y k_y^1)} \\ \vdots \\ \frac{F(k_x^{L-1}, k_y^{L-1})}{\text{Sinc}(w_x k_x^{L-1}) \cdot \text{Sinc}(w_y k_y^{L-1})} \end{bmatrix}_{L \times 1} \\
 &= \vec{b} = A \cdot \vec{v} \\
 &= \begin{bmatrix} e^{-j\pi(k_x^0 \cdot x_0 + k_y^0 \cdot y_0)} & e^{-j\pi(k_x^0 \cdot x_0 + k_y^0 \cdot y_1)} & \dots & e^{-j\pi(k_x^0 \cdot x_{N-1} + k_y^0 \cdot y_{M-1})} \\ e^{-j\pi(k_x^1 \cdot x_0 + k_y^1 \cdot y_0)} & e^{-j\pi(k_x^1 \cdot x_0 + k_y^1 \cdot y_1)} & \dots & e^{-j\pi(k_x^1 \cdot x_{N-1} + k_y^1 \cdot y_{M-1})} \\ \vdots & \vdots & \dots & \vdots \\ e^{-j\pi(k_x^{L-1} \cdot x_0 + k_y^{L-1} \cdot y_0)} & e^{-j\pi(k_x^{L-1} \cdot x_0 + k_y^{L-1} \cdot y_1)} & \dots & e^{-j\pi(k_x^{L-1} \cdot x_{N-1} + k_y^{L-1} \cdot y_{M-1})} \end{bmatrix}_{L \times N \cdot M} \cdot \begin{bmatrix} \alpha_{0,0} \\ \alpha_{0,1} \\ \vdots \\ \alpha_{N-1, M-1} \end{bmatrix}_{N \cdot M \times 1}
 \end{aligned}$$



Idea

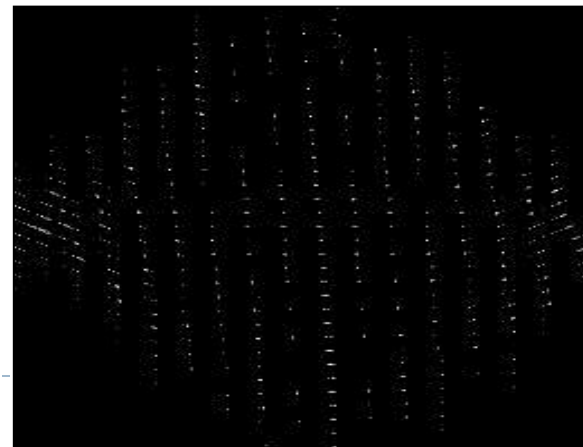
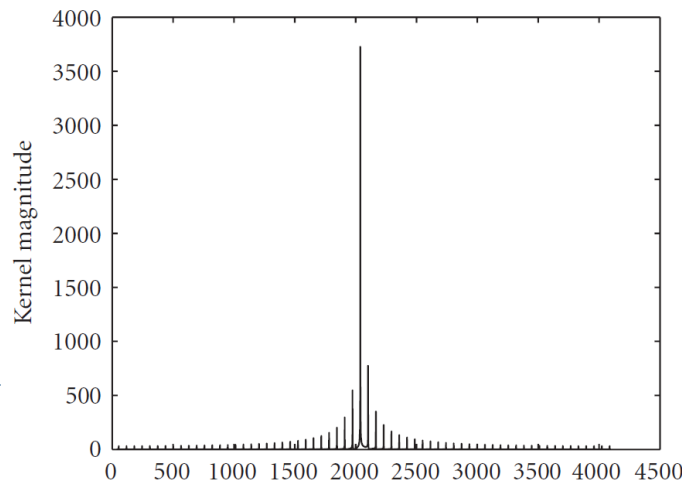
- ▶ Problem: A matrix is dense and computational complexity of solution is prohibitive
- ▶ Solution Strategy: Try to make the A matrix sparse by seeking a compact representation of rows in terms of suitable basis functions
- ▶ Observation: applying a 1-D Fourier transformation to the rows of A matrix results in energy concentration in only a few elements



Methods

- ▶ Multiply the rows of the system matrix by the $N \times M$ -point discrete Fourier transform matrix H in the following form:

$$H = \frac{1}{\sqrt{NM}} \times \begin{bmatrix} 1 & 1 & \dots & 1 \\ 1 & e^{-j2\pi/NM} & \dots & e^{-j2\pi(NM-1)/NM} \\ \vdots & \vdots & \dots & \vdots \\ 1 & e^{-j2\pi(NM-1)/NM} & \dots & e^{-j2\pi(NM-1)^2/NM} \end{bmatrix}_{N \cdot M \times N \cdot M}$$



Methods

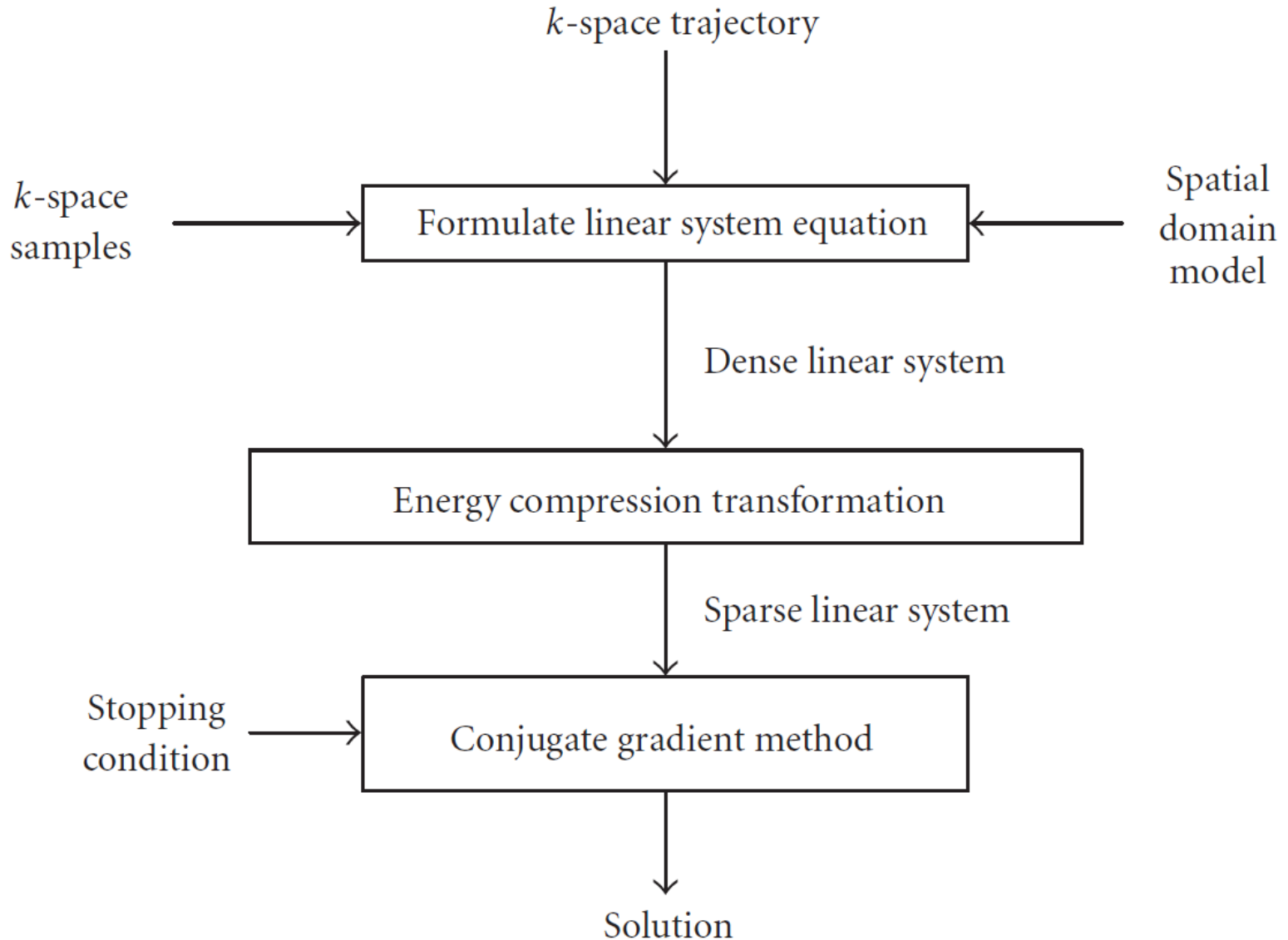
- ▶ How to multiply \mathbf{H} without changing the linear system?
 - ▶ Row energy compacting transformation converts the system into a sparse linear system as follows:

$$b = \mathbf{A}v = \mathbf{A} \cdot \mathbf{H}^H \cdot \mathbf{H} \cdot v = (\mathbf{H} \cdot \mathbf{A}^H)^H \cdot V = \mathbf{M} \cdot V,$$

- ▶ To convert to sparse form, only a percentage η of kernel energy in each row is retained
 - ▶ The only parameter in the new method
 - ▶ Correlates directly to both image quality and computational complexity
- ▶ Sparse matrix techniques are used to store and manipulate the new linear system
 - ▶ Since the linear system is sparse, iterative methods such as conjugate gradient can be used to solve the system with very low complexity



Methods



Results

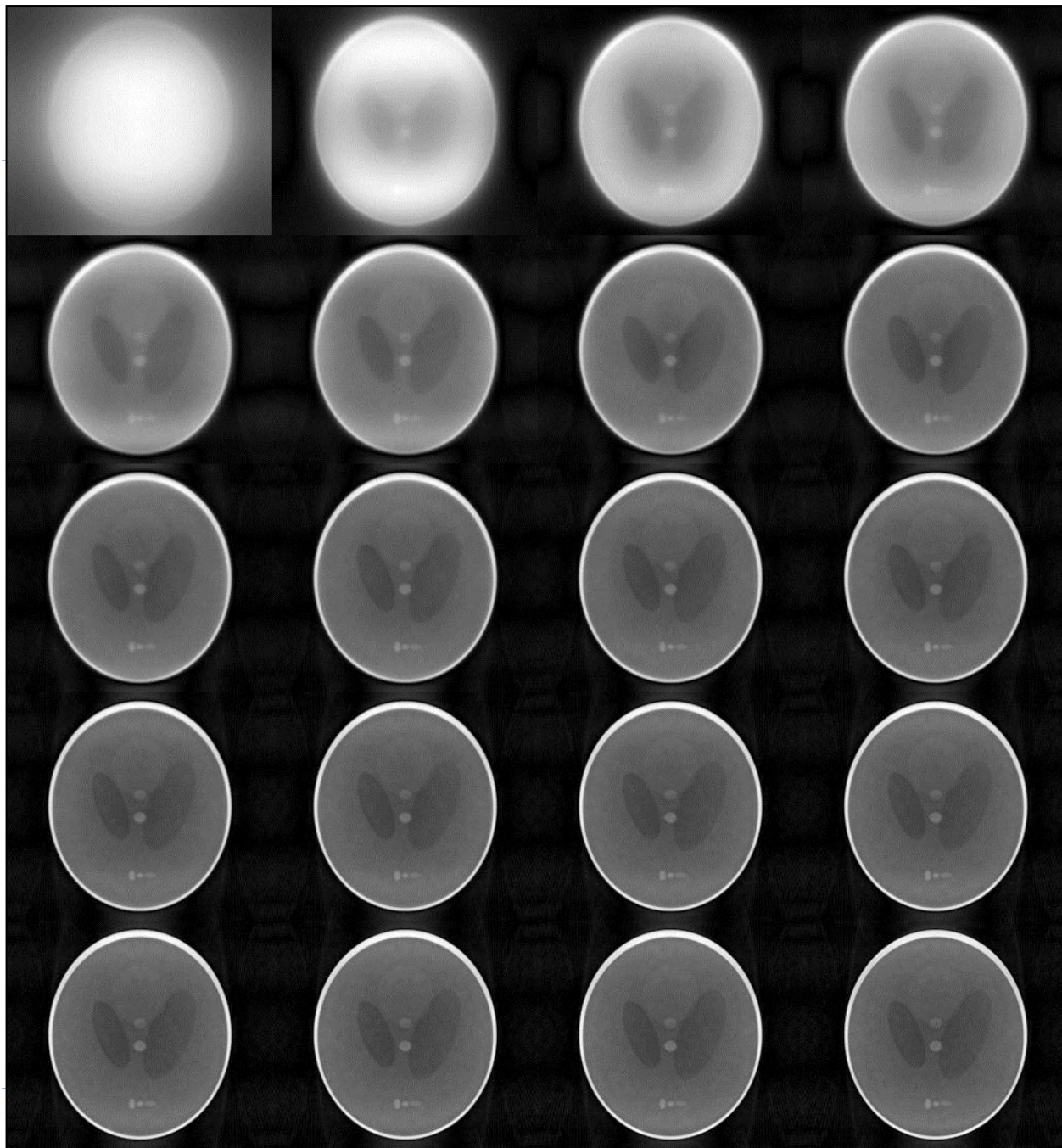
▶ 256x256

Analytical

Shepp-Logan

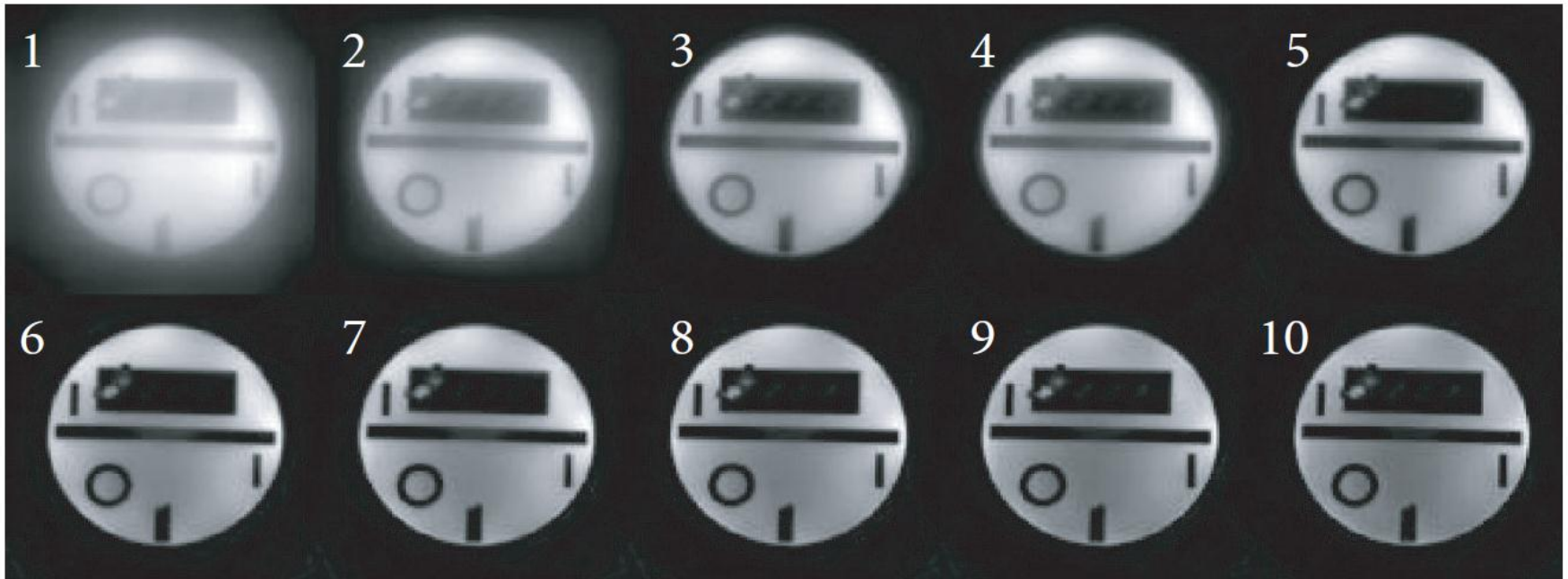
Phantom

(Radial sampling)

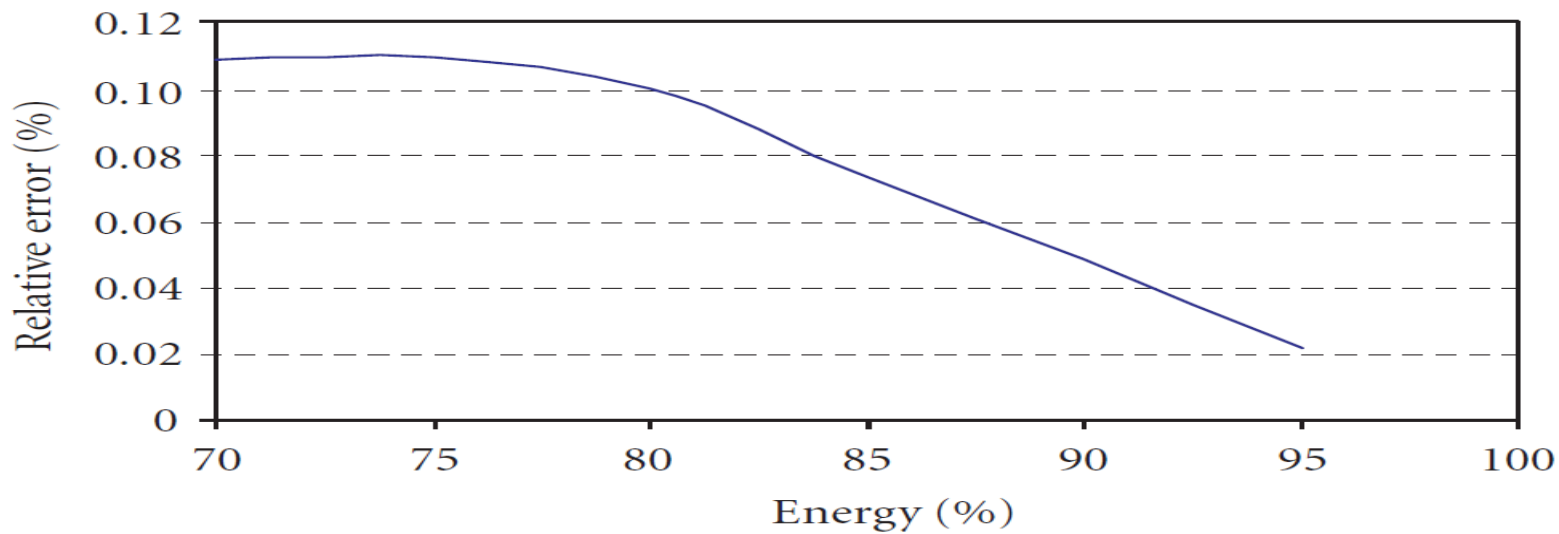
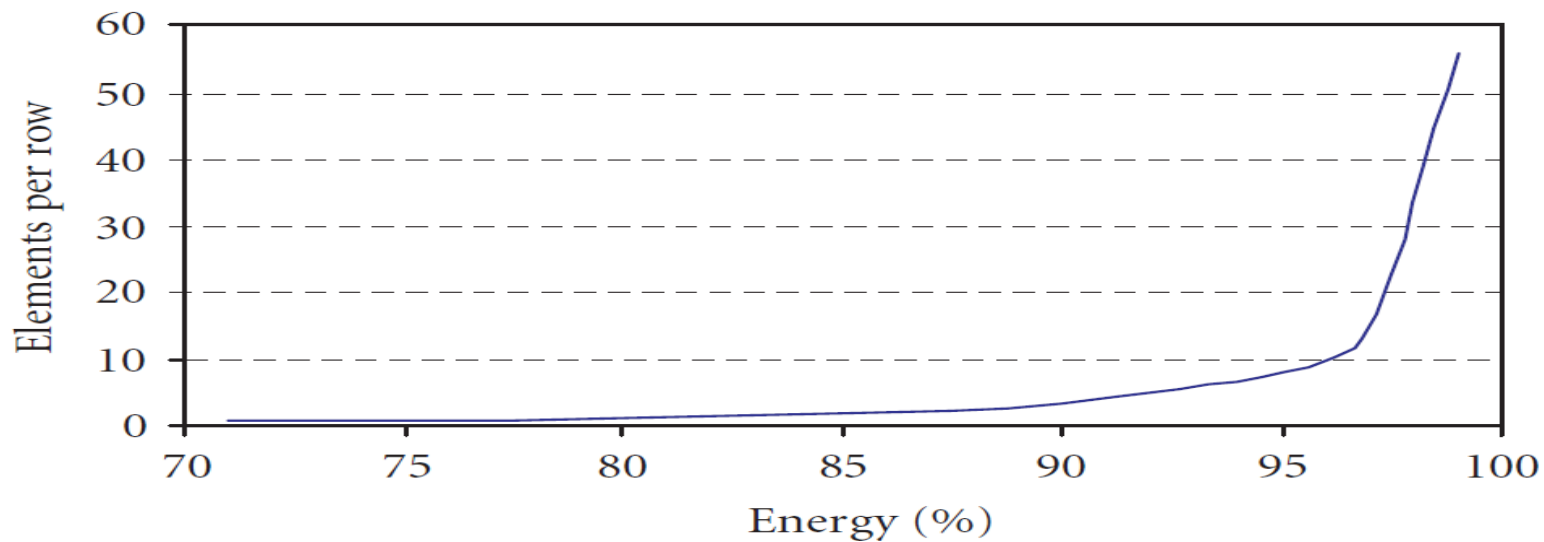


Results

- ▶ 256x256 Real data from a resolution phantom at 3T from a Siemens Magnetom Trio system using a spiral trajectory



Results



Discussion

- ▶ Full control over the accuracy versus complexity trade-off through η selection
- ▶ Computational complexity is comparable to conventional gridding with small kernel
 - ▶ $\mathcal{O}(g(\eta) \cdot L)$ per CGM step, where $g(\eta)$ is the average # of elements/row, $L = \#$ of acquired k-space samples
 - ▶ Average 4.9 elements/row to retain 92% of energy
- ▶ Progressive reconstruction is possible
 - ▶ Add more iterations to process
 - ▶ Use a different reconstruction table with higher η



Exercise

1. Use the MRI data set on the web site and write a program that reconstructs the image using a 2D inverse Fourier transform.
2. Write a program to verify the projection-slice theorem using a simple 2D phantom (e.g., a basic shape like a square).
3. Perform interlaced sampling on a function of your choice with known analytical Fourier transform and verify the interlaced Fourier transform theorem.
4. Write a Matlab program to implement the analytical Shepp-Logan phantom and test it using sampling on a uniform grid.



Exercise

5. Write a short paragraph (less than 500 words) on which partial Fourier reconstruction method you prefer and why.
6. Use the data set on the class web site to implement one of the methods of partial Fourier reconstruction. The data set provided is for full k-space for you to have a gold standard to your reconstruction. You should use only part of it as an input to your reconstruction (say half + 16 lines).
7. Do a literature search on the topic of partial Fourier reconstruction and come up with a list of all references related to the subject.



Exercise

8. Do a literature search on the problem of nonuniform sampling in 2D and summarize your findings about the sampling criteria to avoid aliasing in less than 500 words (in addition to a list of references).
9. Write a program to perform gridding on generated radial k-space sampling of the k-space of the numerical Shepp-Logan phantom to compute the image.
10. In less than 500 words, describe how one can compare the quality of different reconstruction methods and/or parameters based on measurements from the generated images.



Exercise

11. Verify the energy compactness transformation and generate in Kadah's method for any trajectory you prefer.
12. Assuming that we have a rectilinear sampling instead of the nonuniform sampling in this paper, how do you expect the linear system to look like?
13. Assume that we are constructing an $N \times N$ image, compute the exact number of computation (not an order or computation) detailing the list of computations in each step in the implementation.

